

***New Presentations of
Gravity Anomalies
in the Victoria/Bass Strait Region
Page 21***

***Seismic Focus
Interpolation of Horizon Contours
from Sections Sampled from 3D Seismic Data
and from Parallel 2D Seismic Sections
Page 26***

***Conference Review
- Petroleum
Australia's Oil and Gas
- Minerals
Australian Mineral Discoveries - A Question of Scale
Page 9***

***Gamma-ray Spectrometers
Calibration and Use of Portable Gamma-ray Spectrometers
Part 2 - Field Procedures and Calculation of Ground Concentrations
Page 23***

***Resource Investment
Volatility Matters: The Case for Investment in Resource Stocks
Page 31***



Alexander M. Shepherd
Department of
Exploration
Geophysics
Curtin University of
Technology, Perth,
Australia
shephera@geophy.
curtin.edu.au

Allan James
Department of
Geography
University of South
Carolina, USA
AJames@sc.edu

Interpolation of Horizon Contours from Sections Sampled from 3D Seismic Data and from Parallel 2D Seismic Sections

Abstract

This research examines the accuracy of contour maps subsampled from a 3D seismic survey. A 3D seismic data set was interpreted using LANDMARK's "Seisworks-3D" software to build three contour surfaces of stratigraphic horizons at various depths and structural complexities. These horizons were exported and imported to a Geographic Information System (GIS), resampled at various in-line and cross-line, and point spacings, and interpolated to create 3D surface grids from these subsamples of the horizons to simulate interpolation from 2D seismic lines.

In the first set of experiments, for both transect and point data structures, map error decreased as a power function of sample size. This systematic increase in error as sample size decreases allows prediction of the accuracy of interpolation according to sample size and distribution of the data. This relationship facilitates estimation of errors for seismic data interpreters picking a subsample of sections for a particular stratigraphic horizon, determination of receiver and line spacings for sufficient survey accuracy for least economic outlay. Another application of this relationship is to determine the accuracy of interpolative contour mapping on a series of parallel 2D seismic lines according to their spacing.

In a second set of experiments on the point data of a set sample size, map error increased with the local structural complexity of strata sampled. This relationship would allow prediction of the relative precision expected in areas of varying complexity. These findings corroborate earlier work on topographic maps and indicate that similar trade offs between map accuracy and both sample size and surface complexity apply to 3D geological blocks.

Introduction

There has been a lot of cartographic research on the nature of errors associated with sampling strategies. Most studies of sampling errors have been performed on 2D or 2.5D topographic data sets as defined by Raper and Kelk (1991) where there can only be one z value for each x, y coordinate. It has been shown in these studies that higher sampling densities produce more accurate maps, however, the relationship between sampling interval and accuracy is not linear but exponential. For example, MacEachren and Davidson (1987) carried out research to evaluate the effect of sampling density on topographic contour interpolation error. They also examined the effect of the complexity of the interpolated surface on accuracy of the sample. Six topographical surfaces were chosen, each with an empirical value for complexity. Each surface was interpolated 8 times at varying sampling densities expressed in terms of the number of data points: 100, 225, 400, 625, 900, 1225, 1600, and 2025. They found that mean absolute error decreased at a decreasing rate with increasing sampling size. This relationship suggests that for

a given purpose there may be an optimal sample interval at which sufficient relevant information is captured without an excessively large sample. In that experiment, contour maps were interpolated for the same area, from a 1:24 000 topographic sheet that features an eroded syncline dipping to the northeast, located in the Appalachian Mountains, USA. One map was derived using elevations sampled at 50 m intervals in a grid pattern, and the other map was derived using elevations sampled at 500 m intervals. Contour lines interpolated from the points at 50 m intervals clearly portrayed the geology of the area (Maltman, 1990), while on contour maps interpolated from the points at 500 m intervals the geological structural pattern is completely lost.

This research evaluates the interpolation error as it is related to density of sampling of 2D and 3D seismic data sets.

Sampling Interval

The relationship between interpolation accuracy and sampling density is complicated by the complexity of the contour surface. Thus, application of the sampling theorem which states that the sampling interval needs to be less than half the cycle of the highest frequency present in a distribution (Robinson et al., 1995; Brown, 1996; Sheriff, 1991) dictates that increased complexity will require increased sampling densities. In other words, the higher the frequency of change of the subject to be sampled, the closer the samples will need to be spaced to achieve a given accuracy. This is also known as the cardinal theorem or the Nyquist theorem (Sheriff, 1991).

Hypothesis

The hypothesis was tested that errors in interpolated sample grids would be strongly related to the sample size and spacing between picked lines. It was anticipated that there would be an increase in interpolation error as the distance between each of the sample lines was increased. As in the experiments of MacEachren & Davidson (1987), it was hypothesised that the relationship between error and distance between manually picked lines would increase slowly with distance at first but more rapidly with increasing distance; i.e., with decrease in sampling density. The hypothesis was also tested that errors in interpolated sample grids would be related to the structural complexity of the horizon. The three geological horizons that were mapped for this study were thought to require varying sampling densities to capture a given level of map accuracy. This was tested in the experiments.

Methods

Data processing involved the following steps, which are elaborated below. Three master stratigraphic horizons were picked from every in-line and cross-line section on parts of



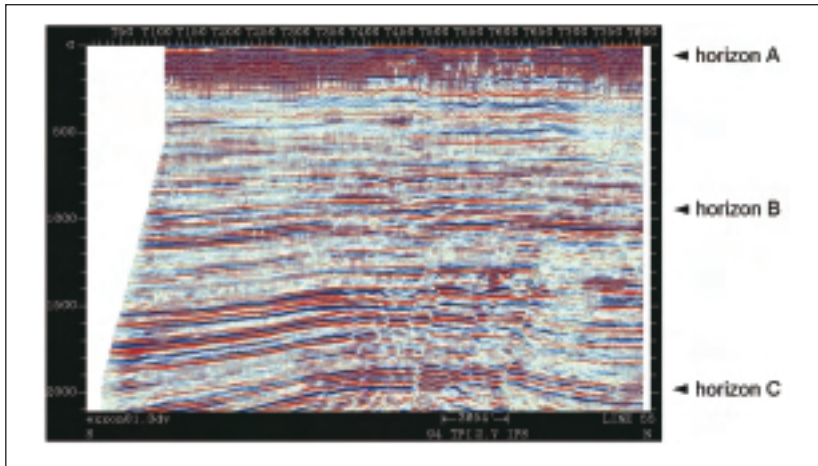
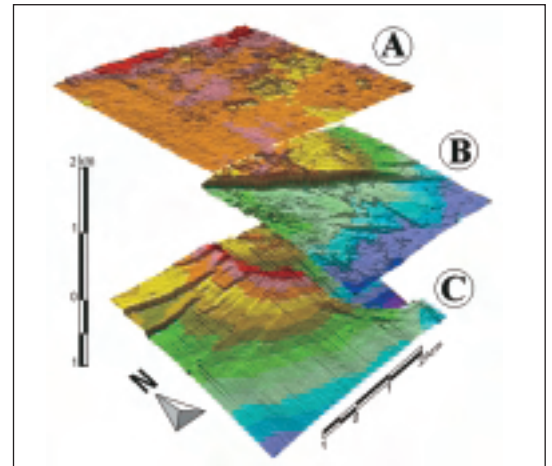


Fig. 1. A part of a north-south cross-section of the Exxon 2D survey in the Gulf of Mexico viewed from the east. Length of section shown is approximately 10 km.

Fig. 2. (Top Right) Perspective view from the south west of the three horizons (A, B, & C) within the 3D seismic block showing various geological complexities including the seismic "footprint" in the data.



the 3D seismic data set with different structural complexities (Figure 1) using LANDMARK's "Seisworks-3D" software (Landmark Graphics Corp., 1998). These master horizons were exported as database files with x, y, z coordinates to the ArcView geographic information system (GIS) (ESRI, 1995) where subsampling and further 2D spatial analysis was conducted including interpolation of contour surfaces and generation of error surfaces and statistics.

In ArcView GIS, the database files were converted into master grid surfaces for each horizon (Figures 2 and 3). Subsamples of x, y, z, data with varying sampling densities (e.g. Figure 4) were selected from the three master grids and were interpolated to create grids with the same area and number of grid cells as the original master grid surface.

The study area is located in South Timbalier in the Gulf of Mexico. The block is approximately 10 km east west by 14 km north south by 10 km deep and is in a thick sequence of sediments deformed by salt diapirs that have pushed up into the upper sediments since the Jurassic Period causing some folding and faulting in the overlying sediments (Rowan and Weimer, 1998; McBride et al., 1998). For this analysis, the master horizons were picked across faults without the introduction of fault surfaces. The horizons sampled were 6.4 km square and contained 65 536 data points arranged as 512 points north south (in-line) by 128 points east west (cross-line).

Anisotropy of Data

The ratio of hydrophone spacing (12.5 m) to streamer spacing (50 m) was of the order of 4:1, so the data array in the original post stack master data set was anisotropic in distribution. This irregular spacing called for special processing (Shepherd, 1999) and two samples were generated for each subsample spacing. These were defined as transect and point samples. Transect samples consisted of complete in-lines and cross-lines but point samples

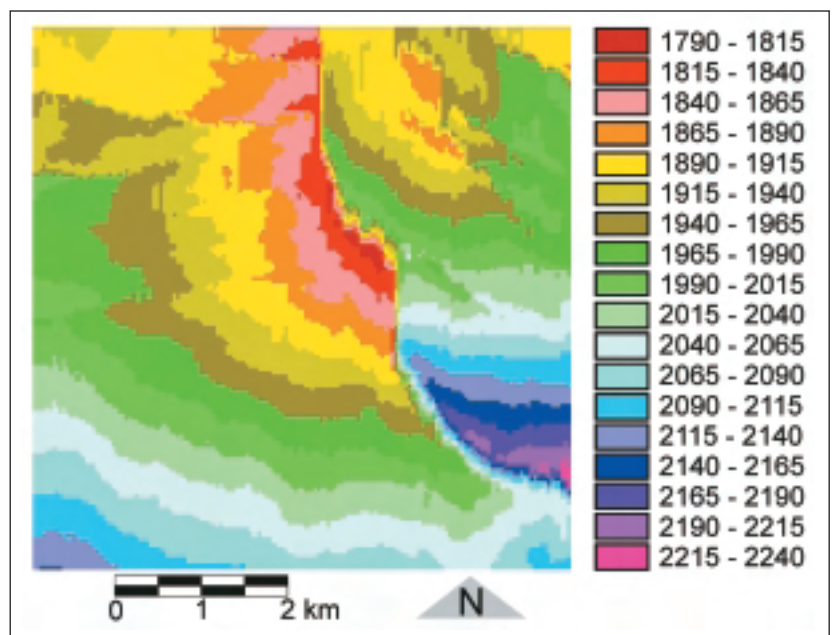


Fig. 3. Master 2.5-D surface for horizon C. Contours show two-way travel times in milliseconds. Number of data points, N, is 65 536

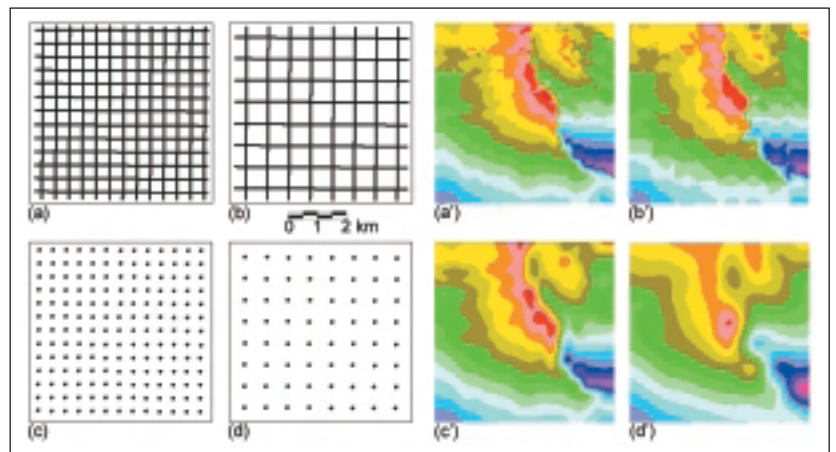


Fig. 4. (Above) Sample grids with corresponding interpolated surfaces for horizon C. For (a), sample size N = 9984, (b), N = 5056, (c), N = 169, and for (d), N = 64. Degree of generalisation increases with increasing line or point spacing. For sample sizes ≤ 169 (c & d) the structural interpretation would change. The discontinuity extending from the north-central edge to the southeast corner of the image is intercepted by an apparent feature trending northeast.

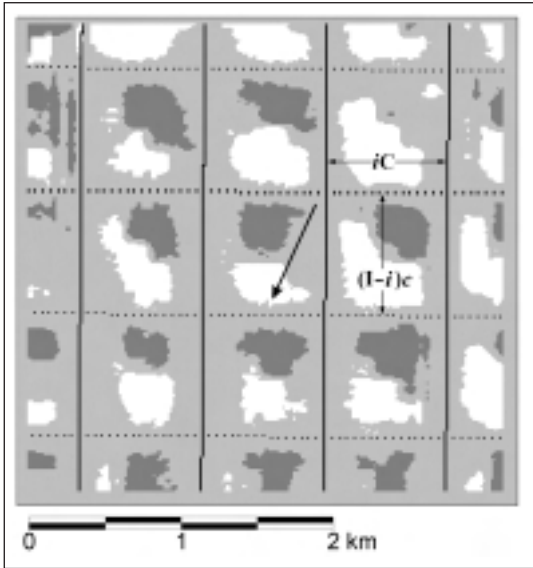


Fig. 5. (Top) Error distribution for transect sample (Fig. 4b) and map (Fig. 4b'). The dark areas are negative error and white areas are positive error. Arrow shows direction of downward slope of horizon C. The parameters for Equation 1 are shown.

Fig. 6. (Above) Cross-section of a difference surface (V) evaluated by subtracting the interpolated surface (U) from the "truth" surface (T). The shaded area (W) shows the absolute difference between the surfaces. The error surface (V) was used to calculate the standard deviation of error statistic and the absolute error surface (W) was used to calculate the mean error statistic.



retained only the intersections (single points in a regular pattern) between the in-lines and cross-lines. Due to anisotropy, sample spacings between in-lines and cross-lines were equal in distance in both orthogonal directions but not equal in number (4:1). It was decided to make the transect sample line numbers isotropic with ratio of 1 north south in-line for every 4th east-west cross-lines or multiples thereof. The transect sample size is arrived at by use of the formula:

$$N = iC + (l - i)c \quad (1)$$

where N is the number of data points in the sample, i is the number of in-lines taken for the sample, c is the number of cross-lines taken for the sample, in these cases, equal to the number of in-lines, l is the number of in-lines in the master horizon data set, and C is the number of cross-lines in the master horizon data set. The

component in the equation $(l - i)$ where i is subtracted from l is necessary to avoid counting the data points at the intersections twice (Figure 5). The values for i and c are obtained by:

$$i = l/n \quad (2)$$

$$c = C/4n \quad (3)$$

where n is the sample spacing for the in-lines. This takes account of the data points included in the cross-lines but not selected in the in-line spacings. 16 sample grids (8 transect and 8 point) were generated from each of the three master horizons. An interpolated grid surface was rendered from each of these 48 sample sets using a spline interpolation algorithm in the ArcView software (ESRI, 1991). The number of cells in each of the interpolated sample grids is on the order of $512^2 = 262,144$ cells, being identical to the number of cells in the master grid surface (Figure 3). The grid cell size (12.5 m) was chosen to match the distance between each in-line hydrophone data point.

It was decided that the spline interpolation algorithm was the most appropriate interpolation method to be used in these experiments. Preliminary tests were carried out on a test point sample, $N=64$ (Figure 4d), to examine the two different algorithms. These were spline and kriging (Dubrule, 1983 and 1984). Results showed that the spline method was more suitable for this project. Hutchison and Gessler (1994) calculated interpolation error by running interpolations with some data points withheld. For each of these interpolations the root mean square error (RMSE) was less for the spline-interpolated surface than for the

equivalent kriged surface. Regardless of which spline interpolation algorithm was used it was assumed that the outcome of this research would not be significantly influenced.

Evaluating Accuracy of Interpolated Horizons

Ehlschlaeger and Goodchild (1994) measured error distribution within a digital elevation model (DEM) by computing the difference between elevations of surveyed data points and elevation of the corresponding DEM pixel. Graphs of the distribution of error showed the effect of error sources. Fischer (1996) evaluated similar error maps. The root mean square error (RMSE) utilised for the tests has often been utilised in cartography to evaluate spatial error in interpolation of spatial data (Morad et al. 1994). Hunter and Goodchild (1995) discuss ongoing research into error modelling in spatial databases.

Each interpolated sample grid surface was subtracted from the corresponding master grid surface (differenced) to obtain an error-grid surface, which maps the magnitude and location of sampling error for each grid point. The statistics for the mean absolute error and the standard deviation of error were calculated, plotted, and analysed to evaluate interpolation accuracy with varying sample densities. Two error grids for each sample size were generated. In the first, the absolute value of error for each cell was mapped. In the second set of error maps, real error was mapped. For each error grid, an overall statistical value was calculated (Figure 6).

Regression of error on sample size and sample spacing was used to examine how errors were related to various sample intervals. Subsamples drawn from the error grids at areas of varying geological complexity were also subjected to regression analysis to evaluate the hypothesis that errors would be related to structural complexity (Figures 7 and 8).

Results

The results of the data interpolation experiments for both transect and point samples clearly demonstrate a decrease in map accuracy as sample size decreases (Table 1). This decreasing accuracy shows up visually on the maps (Figure 4) for horizon C in the form of generalisation. For sample sizes smaller than 169 an apparent northeast-trending

	Horizon A		Horizon B		Horizon C	
Transect Samples						
sample size	mean error	standard deviation	mean error	standard deviation	mean error	standard deviation
36864	0.959	1.708	1.108	2.733	0.917	2.547
19456	1.916	3.22	2.429	5.33	1.981	5.146
12999	2.551	4.201	3.583	7.186	2.862	7.656
9982	3.152	5.185	4.598	9.379	3.962	10.611
8151	3.561	5.671	5.063	10.033	5.202	13.688
6919	3.998	6.31	6.162	12.464	5.591	11.502
5679	4.371	6.731	6.637	12.61	7.342	15.208
5056	4.537	6.837	7.235	13.974	8.07	17.298
Point Samples						
4096	2.408	3.73	2.921	5.896	2.508	6.222
1024	3.663	5.393	4.682	8.289	4.281	9.929
441	4.437	6.311	6.472	10.724	5.934	12.913
256	4.972	6.951	7.768	13.086	7.636	15.938
169	5.508	7.635	9.067	14.918	10.154	20.492
121	6.657	9.155	10.008	16.561	10.159	18.618
81	7.505	10.16	11.654	18.321	12.45	21.668
64	6.923	9.538	13.394	20.758	14.949	26.987

Table 1. Mean and standard deviation statistics for both transect and point samples for all 3 horizons (Shepherd, 1999).

feature is introduced dividing and obscuring the fault that extends across the north-eastern third of the image. The generalisation in these maps would likely lead to an entirely different structural interpretation than with use of maps derived from full resolution data.

When "standard deviations of error" are plotted against "sample size" for the transect samples (Figure 7) and the point samples (Figure 8), the systematic decrease in error with increase in sample size becomes clear. Trend lines were calculated by least squares computational methods for both the mean absolute error and the standard deviation of error in the three horizons. The best-fit trend lines were determined by maximum explained variance (R^2) values and graphical evaluation of regression residuals using various univariate models. Power functions fit best for Horizons B and C, but the best fits for Horizon A for both, the transect and point samples, for the standard deviation statistic, were logarithmic functions. Horizon A had less concavity (on linear scales) to the error versus sample size trend than the other two horizons, presumably reflecting the simple nature of the stratigraphic structure.

A comparison was made between the standard deviation of error for Horizons A, B, and C. There were substantial differences in the standard deviation statistics between the horizons, probably due to varying geological complexity between the horizons. Horizon A has no faults but may have a higher frequency of data while Horizons B and C each have faults of differing relief or throws. There was a greater decrease in accuracy with structural complexity for the point samples than for the transect samples (Figure 4a' and 4b'). If only power functions are considered then a possible trend between their constants and exponents can be analysed. This is justified because the regressions are all fairly strong with $R^2 > 0.97$ for all values. The general form of the power function is:

$$E = a N^{-b} \quad (4)$$

Where E is interpolation error, N is sample size, a is a constant representing the standard deviation of error at $N=1$, and b is an exponent expressing the rate of change in log E with log N.

The fact that the relationship between sample size and error, is inverse and alters exponentially is supported by the negative values ($b < 1$) of the exponent b in the power functions. For the transect samples, the value of b ranges from -0.697 (horizon A) to -0.945 (horizons C) respectively, probably due to the much larger sample sizes whereas, for the point samples, the values are lower, being from -0.237 (horizon A) to -0.337 (horizon C), for the much smaller sample sizes. The distribution of the sampled data points could also be a factor and would require further investigation. The difference between the values of the constant a for the transect and the point samples is very great, likely due to sample data distribution as well as size (Table 2).

	Horizon A	Horizon B	Horizon C
Transect Samples			
constant a	2907.8	15156	56984
exponent b	-0.6965	-0.8114	-0.9448
Point Samples			
constant a	26.975	70.48	102.59
exponent b	-0.2371	-0.3033	-0.3368

Table 2. Relationship between the constant a and the exponent b for all 3 horizons.

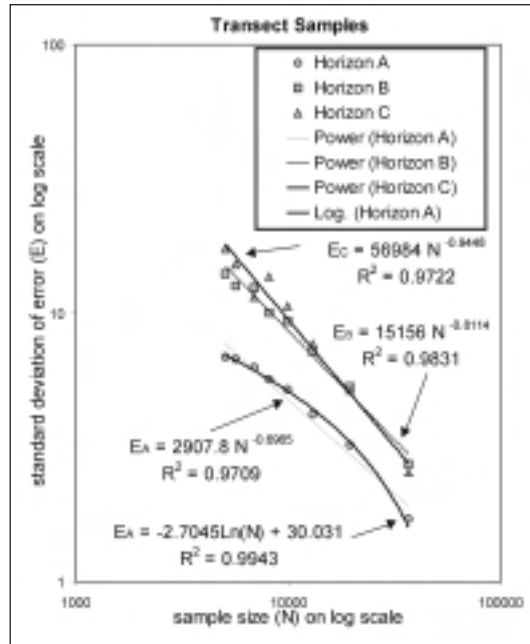


Fig. 7. Regression analysis for transect samples showing relationship between transect sample size and standard deviation of error plotted on logarithmic scales on both axes.

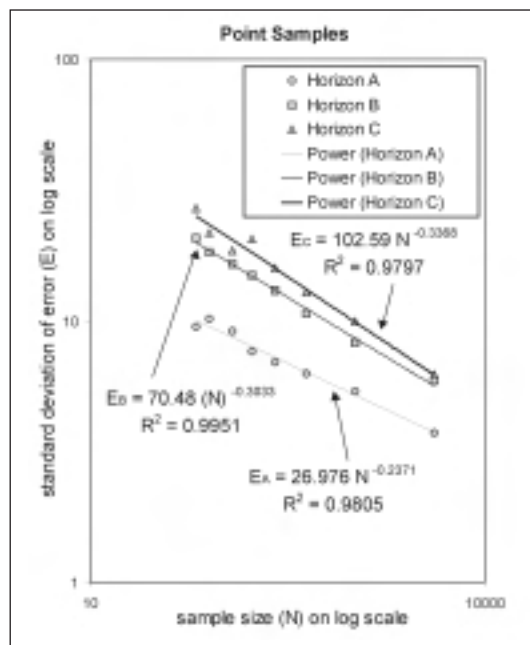


Fig. 8. Regression analysis for point samples showing relationship between transect sample size and standard deviation of error plotted on logarithmic scales on both axes.

For the standard deviation of error, values of the constant a and exponent b in Equation 4 show an apparent trend that supports the second hypothesis that error increases with structural complexity. Based on three sample-horizon experiments, values of a and b increase in value from horizons A to C. This empirical relationship appears to be linear for both the constant and the exponent in the point samples and for the exponent in the transect samples but is exponential for the constant in the transect samples (Shepherd, 1999). Although more experiments are needed to validate the relationship, this trend corresponds with increasing structural complexity.

One application for these results is to determine the interpolation accuracy of a series of parallel 2D seismic lines at equal intervals. For example parallel 2D lines were surveyed north of the Stag Oil Field in the Eastern Dampier Sub-Basin off the coast of Western Australia with a line



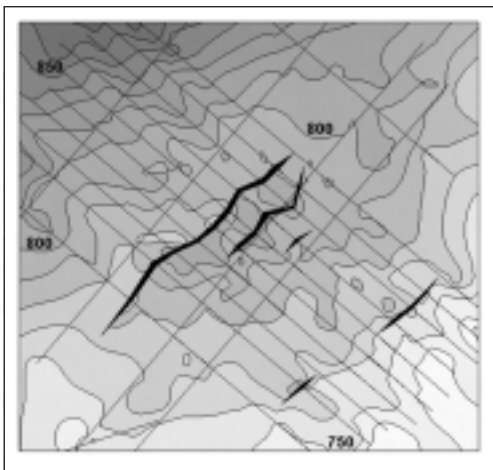


Fig. 9. Arrangement of parallel seismic sections from a 2D survey north of the Stag Oil Field in the Eastern Dampier Sub-basin off the coast of Western Australia. Closest line spacing is approximately 500 m.

Conclusions

In two-dimensional analyses, it has previously been shown that map accuracy varies inversely with sample size on the one hand, and with the combination of sample size and feature complexity on the other. This study presents evidence that these relationships also apply to the accuracy of mapping three-dimensional features. Furthermore, this study provides a basis for quantifying this relationship. As hypothesised, the rate of decrease in interpolation error decreased with increase in sample size. This was found to be true for both types of sample sets: points and transects and corroborates the findings of MacEachren and Davidson (1987). However, there was a greater change in the rate of decrease in mean error and standard deviation of error for the point samples than for the transect samples. This is supported by the values of the exponent b in the power functions.

Sample size is not the only criterion that determines interpolation accuracy. The distribution of the data points also has to be taken into account. For example, the smallest transect sample size ($N=5056$) and the largest point sample size ($N=4096$) are similar in terms of sample size alone but radically different in terms of data point distribution.

The hypothesis that error increases with structural complexity is also supported by the analysis. The mean absolute error and the standard deviation are greater for horizons B and C than for horizon A. This is presumably because horizon A has no faults and a lower range of two-way travel times. All the graphs show a curvilinear trend (a nearly straight line on logarithmic scales) of summary errors (mean absolute or standard deviation) versus sample size (transect or point) where the slope is steepest at the smaller sample sizes. Power functions with a negative exponent fit most of these trends quite well.

Acknowledgments

The authors wish to thank Prof. Christopher Kendall (Department of Geology), and Dr. Robert Lloyd (Department of Geography) of the University of South Carolina, USA and many others for their input and assistance in this research and also to LANDMARK Corp. and the Environmental Systems Research Institute (ESRI) for provision of the software. This research was completed using the computer facilities in the Department of Exploration Geophysics at Curtin University of Technology in Perth, Western Australia.

spacing of approximately 500 metres (Figure 9); equivalent to the transect sample spacing shown by the grid (a) and the map (a') in Figure 4. Two-way travel time contours were interpolated using the LANDMARK Seisworks package. We can determine the accuracy of interpolation of this example from the regression analysis (Figure 7) and obtain an estimate of errors in the calculations of such things as volume of oil or gas in place and factor this into risk analysis assessments.

References

- Brown, A. R., 1996, Interpretation of Three-Dimensional Seismic Data (Memoir 42, 4th edition), American Association of Petroleum Geologists (AAPG), Tulsa, OK.
- Dubrule, O., 1983, Two Methods with Different Objectives: Splines and Kriging: *Mathematical Geology*, 15, 245-257.
- Dubrule, O., 1984, Comparing Splines and Kriging: *Computers & Geosciences*, 10, 327-338.
- Ehlschlaeger, C. R. and Goodchild, M. F., 1994, Uncertainty in Spatial Data: Defining, Visualizing, and Managing Data Errors: *Proceedings of GIS / LIS '94*.
- Environmental Systems Research Institute (ESRI), 1991, Grid Command References: instruction manual.
- Environmental Systems Research Institute, 1995, Understanding GIS, The Arc/Info Method: instruction manual.
- Fischer, P. F., 1996, Animation of Reliability in Computer-generated Dot Maps and Elevation Models: *Cartography and Geographic Information Systems*, 23, 196-205.
- Hunter, G. J. and Goodchild, M. F., 1995, Dealing with Error in Spatial Databases: A simple case Study: *Photogrammetric Engineering and Remote Sensing*, 61, 529-537.
- Hutchison, M. F. and Gessler, P. E., 1994, Splines - more than just a smooth interpolator: *Geoderma*, 62, 45-67.
- Landmark Graphics Corp., 1998, Seisworks 3D: user's instruction manual.
- MacEachren, A. M. and Davidson, J. V., 1987, Sampling and Isometric Mapping of Continuous Geographic Surfaces: *The American Cartographer*, 14, 335-343.
- Maltman, Alex, 1990, Geological Maps - an Introduction, Chapter 8, 84-92, Open University Press, Milton Keynes, UK.
- McBride, B. C., Rowan, M. G. and Weimer, P., 1998, The Evolution of Allochthonous Salt Systems, Northern Green Canyon and Ewing Bank (Offshore Louisiana), *Northern Gulf of Mexico: AAPG Bulletin*, 82, 1013-1036.
- Morad, M., Chalmers, A. I., and O'Regan, P. R., 1996, The role of root-mean-square error in the geo-transformation of images to GIS: *International Journal of Geographic Information Systems*, 10, 347-353.
- Raper, J. F. & Kelk, B., 1991, Three-dimensional GIS, *Geographical Information Systems: in Geographical Information Systems* edited by Maguire, D. J., Goodchild, M. F. & Rhind, D. W., 1, 299-317, Longman Scientific and Technical, Harlow, Essex, England, and J. Wiley & Sons, New York.
- Robinson, A. H., Morrison, J. L., Muehrcke, P. C., Kimmerling, A. J., & Gupthill, S. C., 1995, *Elements of Cartography* (sixth edition), Chapter 26, 497-526, J. Wiley & Sons, New York.
- Rowan, Mark G., and Paul Weimer, 1998, Salt-Sediment Interaction, Northern Green Canyon and Ewing Bank (Offshore Louisiana), *Northern Gulf of Mexico: AAPG Bulletin*, 82, 1055-1082.
- Shepherd, A. M., 1999, Accuracy of interpolations for geological mapping made from 3-D seismic models using a geographic information system: Unpublished Masters of Science Thesis, Department of Geography, University of South Carolina, USA.
- Sheriff, R. E., 1991, *Encyclopedic Dictionary of Exploration Geophysics* (third edition): Society of Exploration Geophysicists.

